

## RED FLUORESCENT LINE EMISSION FROM HYDROGEN MOLECULES IN DIFFUSE MOLECULAR CLOUDS

DAVID A. NEUFELD AND MARCO SPAANS

Department of Physics and Astronomy, The Johns Hopkins University, Baltimore, MD 21218

Received 1996 March 11; accepted 1996 July 9

### ABSTRACT

We have modeled the fluorescent pumping of electronic and vibrational emissions of molecular hydrogen ( $H_2$ ) within diffuse molecular clouds that are illuminated by ultraviolet continuum radiation. Fluorescent line intensities are predicted for transitions at ultraviolet, infrared, and red visible wavelengths as functions of the gas density, the visual extinction through the cloud, and the intensity of the incident UV continuum radiation. The observed intensity in each fluorescent transition is roughly proportional to the integrated rate of  $H_2$  photodissociation along the line of sight. Although the most luminous fluorescent emissions detectable from ground-based observatories lie at near-infrared wavelengths, we argue that the lower sky brightness at visible wavelengths makes the red fluorescent transitions a particularly sensitive probe. Fabry-Perot spectrographs of the type that have been designed to observe very faint diffuse  $H\alpha$  emissions are soon expected to yield sensitivities that will be adequate to detect  $H_2$  vibrational emissions from molecular clouds that are exposed to ultraviolet radiation no stronger than the mean radiation field within the Galaxy. Observations of red  $H_2$  fluorescent emission together with cospatial 21 cm  $H\text{ I}$  observations could serve as a valuable probe of the gas density in diffuse molecular clouds.

*Subject heading:* infrared: ISM: lines and bands — ISM: molecules — molecular processes — ultraviolet: ISM

### 1. INTRODUCTION

Vibrational emissions from hydrogen molecules have been widely observed from molecular clouds both in the Milky Way (e.g., Shull & Beckwith 1982; Beckwith et al. 1978; Gatley et al. 1987; Chrysostomou et al. 1993) and in other galaxies (e.g., Kawara, Nishida, & Gregory 1987; Doyon, Wright, & Joseph 1994). Such observations have been carried out primarily at near-infrared wavelengths, particularly in the  $K$  atmospheric window (2–2.5  $\mu\text{m}$ ) where much of the  $H_2$  vibrational emission emerges in the fundamental ( $\Delta v = 1$ ) bands. Vibrational emission from  $H_2$  has also been detected at shorter wavelengths from the Orion molecular cloud in the  $v = 2-0$  band near 1  $\mu\text{m}$  (Münch, Hippelein, & Pitz 1984; Hippelein & Münch 1989), as well as from the reflection nebula NGC 2023 in the 0.76–0.88  $\mu\text{m}$  (“far-red”) spectral region (Burton et al. 1992; see also the upper limits obtained in this spectral region by Gull & Harwit 1971 and Traub, Carleton, & Black 1978 toward several sources).

Sensitive observations of extended regions (Luhman et al. 1994; Pak, Jaffe, & Keller 1996) suggest that fluorescent pumping by ultraviolet radiation is the dominant mechanism responsible for the excitation of  $H_2$  vibrational emissions within the Milky Way, although collisional excitation appears to be primarily responsible for such emissions in localized outflow regions where shock waves warm the gas to temperatures greater than 1000 K (Draine & Roberge 1982; Chernoff, Hollenbach, & McKee 1982). While space-based observatories have been used to detect fluorescently pumped ultraviolet electronic transitions of  $H_2$  molecules within the diffuse interstellar medium (Martin, Hurwitz, & Bowyer 1990, hereafter MHB90), observations of fluorescent  $H_2$  vibrational emissions (accessible from the ground) have been limited to relatively *dense* molecular clouds that are illuminated by ultraviolet radiation fields substantially stronger than the mean interstellar radiation field within the Galaxy. However, recent developments in observational

capabilities promise to yield sensitivities that will be adequate to detect  $H_2$  vibrational emissions from *diffuse* molecular clouds that are exposed to ultraviolet radiation no stronger than the mean radiation field within the Galaxy. Such observations may ultimately be possible at near-infrared wavelengths or—as we argue in this paper—at red visible wavelengths, using Fabry-Perot spectrographs of the type that have been designed to observe very faint diffuse  $H\alpha$  emissions (Vogel et al. 1995).

Not surprisingly, theoretical efforts to model  $H_2$  fluorescence (e.g., Black & Dalgarno 1976, hereafter BD76; Black & van Dishoeck 1987, hereafter BvD87; Sternberg & Dalgarno 1989, hereafter SD89; Draine & Bertoldi 1996, hereafter DB96) have generally emphasized line emission in the near-infrared spectral region longward of 1  $\mu\text{m}$ , where most of the observations have been carried out, and, with the exception of BD76, where they have been applicable to “dense” rather than “diffuse” molecular clouds (i.e., to clouds of large visual extinction that absorb essentially all the ultraviolet radiation that is incident upon them.) In this paper, we have extended the work of BD76 by carrying out a general parameter study of fluorescent  $H_2$  vibrational line emissions from diffuse molecular clouds. We present predictions for such emissions for clouds with H nuclei densities in the range 50–1000  $\text{cm}^{-3}$  and visual extinctions extending to the regime  $A_V \leq 1$ . While the brightest near-infrared  $H_2$  vibrational lines (with  $\Delta v = 1$ ) are expected to be more luminous than visible wavelength transitions (with  $\Delta v \geq 3$ ) by an order of magnitude or more, the lower sky brightness at visible wavelengths makes red  $H_2$  transitions a particularly sensitive probe, as noted by BD76. Accordingly, we emphasize the predicted line intensities for transitions in the 0.6–1.0  $\mu\text{m}$  range.

In § 2, we describe our calculation of the  $H_2$  fluorescent emission expected from a spherical molecular cloud that is exposed to an external UV radiation field. In § 3, we present the results of a general parameter study in which the depen-

dence of the H<sub>2</sub> line intensities upon the incident radiation field, the gas density, and the cloud diameter was investigated. In § 4, we discuss current observational capabilities and argue that observations of red H<sub>2</sub> fluorescent emission together with cospatial 21 cm H I observations could serve as a valuable probe of the gas density and dust content in diffuse molecular clouds. We also discuss the interpretation of previous ultraviolet observations of fluorescent *electronic* transitions of H<sub>2</sub>.

## 2. CALCULATIONS

We have constructed models to compute the H<sub>2</sub> fluorescent line intensities expected from diffuse molecular clouds. The excitation of vibrational line emission results from pumping of the Lyman and Werner bands of H<sub>2</sub> by UV radiation in the 912–1107 Å region (Gould & Harwit 1963), followed by radiative decay to the ground electronic state. The fluorescent excitation of vibrational line emission is intimately linked to the photodissociation of H<sub>2</sub> (Solomon 1965, attributed by Field, Somerville, & Dressler 1966; Stecher & Williams 1967; Stephens & Dalgarno 1972), since approximately 15% of Lyman and Werner band excitations are followed by spontaneous radiative dissociation rather than radiative decay to the ground electronic state.

Our treatment of the pumping and dissociation of molecular hydrogen by ultraviolet radiation follows closely the detailed calculations described by BvD87, by SD89, and DB96. We included the radiative pumping by ultraviolet radiation of all Lyman and Werner band transitions involving states of rotational quantum number,  $J \leq 14$ . The self-shielding in each transition was considered individually using an approximation to the escape probability based upon expressions given by Tielens & Hollenbach (1985). The effects of line overlap were not included but are not expected to be important for the conditions of present interest. Full details of our calculation will be described in a future paper, but the significant differences between our treatment of H<sub>2</sub> pumping and dissociation and that adopted in previous studies can be summarized as follows:

1. In contrast to each of the previous studies cited above, we assumed the molecular hydrogen to lie in a spherical cloud that is illuminated by an isotropic radiation field, rather than in a plane-parallel slab that is illuminated from one direction by a single UV source. The spherical geometry that we adopted here—also considered recently by Störzer, Stutzki, & Sternberg (1996) in their model for carbon chemistry within dense clumps inside molecular clouds—is more appropriate to the diffuse clouds of present interest.

2. In contrast to the models of SD89 and DB96, we neglected the collisional de-excitation of excited vibrational states. This simplification is justified because of the low cloud densities ( $n_{\text{H}} \leq 1000 \text{ cm}^{-3}$ ) considered in this work. We included collisional excitation within the ground vibrational state, adopting the recommendations of Lepp, Buch, & Dalgarno (1995) for the rate coefficients for the excitation of H<sub>2</sub> rotational states in collisions with H.

3. We did not include the reactive collisions that may lead to ortho and para conversion in molecular clouds. Instead, we adopted a fixed ortho-to-para ratio of 1.0, the average value indicated by *Copernicus* observations of diffuse molecular clouds (Savage et al. 1977).

4. We did not include the “formation pumping” that

results from the grain-catalyzed formation of H<sub>2</sub> molecules in excited ro-vibrational states. The total H<sub>2</sub> line luminosity resulting from formation pumping is small compared to the total fluorescent emission, but specific transitions (particularly those that are not pumped efficiently by fluorescence) might be substantially enhanced. Because the initial excitation state of newly formed H<sub>2</sub> molecules remains rather uncertain, our philosophy has been to neglect formation pumping so as not to risk overestimating the strengths of particular transitions. Thus, we assume that if radiative excitation from a given state ( $v, J$ ) of the ground electronic state is followed by spontaneous radiative dissociation, the subsequent reformation of an H<sub>2</sub> molecule will take place into the identical ro-vibrational state ( $v, J$ ). This conservative approach might lead to underestimates of the predicted strengths for transitions that are particularly favored by formation pumping, but it has the advantage that a prediction that a particular line is observable will never rest upon a grain formation model that may turn out to be wrong.

As in the previous studies cited above, we have assumed chemical equilibrium, with the rate of H<sub>2</sub> formation equal to the rate of photodissociation. This assumption would lead to an over/underestimate of the fluorescent line intensities if the actual rate of photodissociation were smaller/larger than the rate of molecule formation (Goldshmidt & Sternberg 1995). We also follow previous studies in neglecting the effect of resonance fluorescence in transitions leading to the ground vibrational state, and in making use of the quadrupole transition probabilities of Turner, Kirby-Docken, & Dalgarno (1977) in computing the radiative cascade within the ground electronic states; unfortunately, these transition probabilities are not expected to be particularly accurate (Dalgarno 1996)—especially for transitions with  $\Delta v > 1$ —because the results depend very sensitively upon the details of the assumed quadrupole moment function,  $Q(R)$ .

By an iterative procedure, we determined the photodissociation rate, pumping rates, equilibrium H<sub>2</sub> abundance, and H<sub>2</sub> level populations at each point within a spherical cloud of uniform density  $n_{\text{H}}$  (H nuclei per unit volume) and diameter  $d$ , which is exposed to a uniform radiation field with an intensity of  $I_{\text{UV}}$  times the mean interstellar value adopted by Draine (1978). Then we computed the emergent vibrational line intensities for a ray that passes along the diameter of the cloud. We included the effects of dust attenuation for both the incident UV radiation and the emergent fluorescent radiation. To check our treatment of H<sub>2</sub> pumping and dissociation, we also computed the fluorescent line intensities expected from a plane-parallel slab with the parameters adopted by BvD87 in their model 1. Our results agreed to within 15% for each of the 36 ro-vibrational line intensities presented in Table 2 of BvD87, and the total fluorescent intensities agreed to better than 3%. To facilitate an additional check, B. Draine kindly provided us with line-strength predictions generated by the model of DB96 for the case of a plane-parallel “diffuse cloud” with  $A_V = 0.2$  mag,  $I_{\text{UV}} = 1$ , and  $n_{\text{H}} = 100 \text{ cm}^{-3}$ . For all the red H<sub>2</sub> transitions considered in this paper, the maximum disagreement was  $\sim 12\%$ , and the typical (i.e., median) discrepancy was only 4%.

In all of our spherical cloud models, we assumed a gas temperature of 77 K, such that reactive collisions between

$\text{H}_2$  and  $\text{H}_3^+$  or  $\text{H}^+$  atoms lead to the ortho-to-para ratio of unity that is typical of diffuse clouds (Savage et al. 1977). We adopt a Doppler parameter for the  $\text{H}_2$  lines of  $3 \text{ km s}^{-1}$  and assume that  $\text{H}_2$  formation is catalyzed by dust grains at a rate per unit volume of  $Rn_{\text{H}}n(\text{H})$ , where  $3 \times 10^{-17} \text{ cm}^3 \text{ s}^{-1}$  is the assumed value of  $R$  and  $n(\text{H})$  is the density of H atoms. We assumed that the ratio of visual extinction,  $A_V$ , to the column density of H nuclei,  $N_{\text{H}}$ , was  $5.9 \times 10^{-22} \text{ mag cm}^2$ . The parameters we varied were  $n_{\text{H}}$  (over the range  $50\text{--}1000 \text{ cm}^{-3}$ ),  $I_{\text{UV}}$  (taken as 1 or 5), and the total visual extinction through the cloud,  $A_V = 5.9 \times 10^{-22} n_{\text{H}} d \text{ mag}$  (for which we considered values as small as 0.01).

### 3. RESULTS

The line intensities predicted by our model are shown in Figures 1 and 2 for two representative transitions: the infrared  $v = 1\text{--}0 \text{ S}(1)$  line at  $2.122 \mu\text{m}$  and the visible wavelength  $v = 6\text{--}2 \text{ S}(2)$  line at  $7180.5 \text{ \AA}$ . The  $v = 1\text{--}0 \text{ S}(1)$  line is one of the brightest and best-studied near-infrared lines, while the  $v = 6\text{--}2 \text{ S}(2)$  line is one of the brighter visible wavelength lines. Figure 1 applies to the case  $I_{\text{UV}} = 1$ , and Figure 2 applies to the case  $I_{\text{UV}} = 5$ . Solid lines in these figures show the intensity of the radiation, integrated over each line, for rays that traverse the cloud diameter. Results are shown as a function of the atomic hydrogen column density along the ray,  $N(\text{H})$ , and for several values of  $n_{\text{H}}$ . Dashed curves connect models of the same total  $A_V$ . We also present the total fluorescent UV intensity over the entire  $1400\text{--}1700 \text{ \AA}$  range, for comparison with space-based observations of

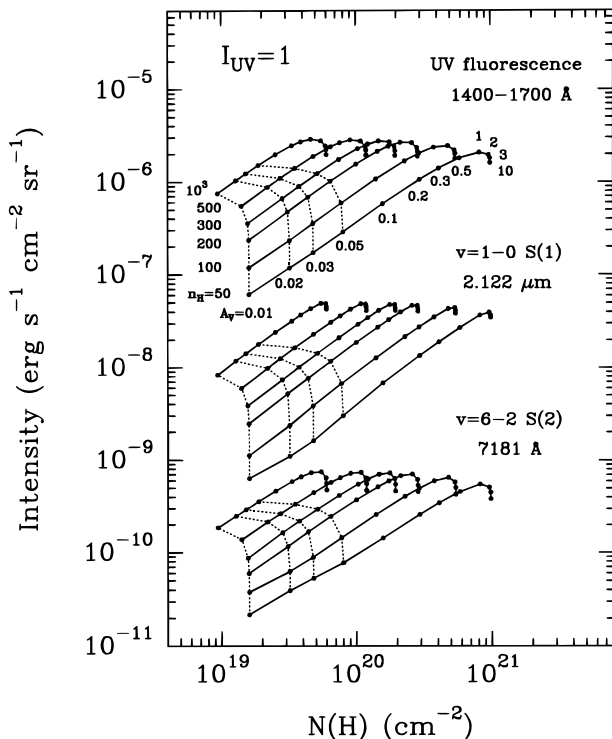


FIG. 1.—Solid lines: fluorescent line intensities—as functions of atomic hydrogen column density—for several values of the density of H nuclei. Results apply to the case ( $I_{\text{UV}} = 1$ ) when the incident UV continuum radiation field is equal to that adopted by Draine (1978). Dashed lines connect models with the same total visual extinction across the cloud diameter.

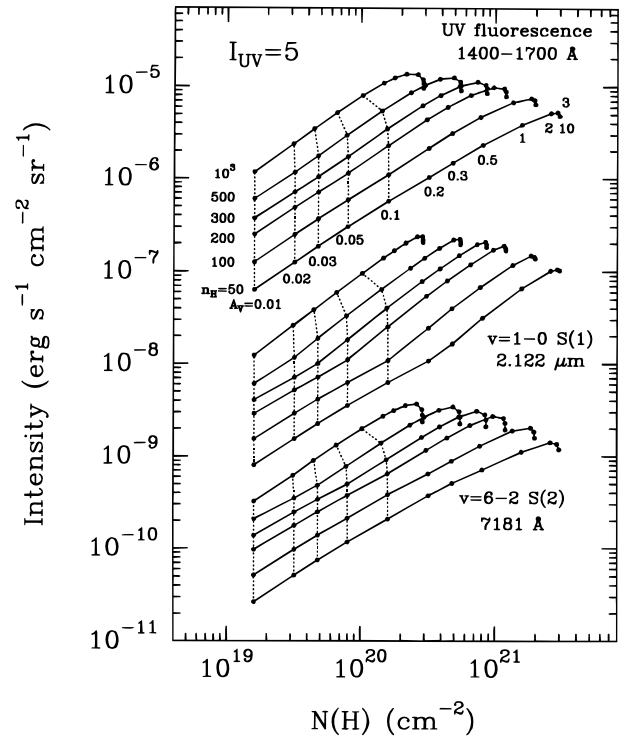


FIG. 2.—Same as Fig. 1, except for an incident UV continuum radiation field 5 times as large ( $I_{\text{UV}} = 5$ ).

fluorescently pumped electronic transitions. Our calculation of the  $1400\text{--}1700 \text{ \AA}$  intensities includes both fluorescent line emission and the continuum emission associated with spontaneous radiative dissociation.

Our choice of  $N(\text{H})$  as the independent variable in Figures 1 and 2 is motivated by two considerations. First,  $N(\text{H})$  (unlike  $N(\text{H}_2)$  or  $A_V$ ) is a quantity that can be directly and reliably measured by means of 21 cm observations along any line of sight in a diffuse cloud. Second, the figures as plotted demonstrate explicitly that the fluorescent line intensities are roughly proportional to the quantities  $N(\text{H})$  and  $n_{\text{H}}$ . This behavior arises because of the intimate connection between fluorescence and photodissociation. Because the rates of these processes decline in the same manner as the degree of self-shielding increases, the amount of energy generated in any given transition maintains a roughly constant value,  $E$ , per molecule dissociated. In chemical equilibrium, with the molecule formation rate equal to the photodissociation rate, the integrated line intensity therefore traces the rate of molecule formation integrated along the ray, and it may be written

$$I_f = \frac{Rn_{\text{H}}N(\text{H})\bar{E}(1-f_a)}{4\pi}, \quad (1)$$

where  $\bar{E}$  is the mean value of  $E$  along the line of sight. The quantity  $f_a$  is the (wavelength-dependent) fraction of fluorescent photons emitted along the line of sight that are absorbed by dust before they can escape the cloud. Over a wide range of model parameters,  $\bar{E}$  is roughly constant, so the proportionality  $I_f \propto n_{\text{H}}N(\text{H})$  applies approximately in the low column density regime where  $f_a \ll 1$ . At large column densities, dust absorption becomes important and

TABLE 1  
H<sub>2</sub> FLUORESCENT EMISSION: ENERGY EMITTED  
PER PHOTODISSOCIATION FOR  
SELECTED TRANSITIONS

Transition ( <i>v</i> )	Wavelength (Å)	$\bar{E}$ (ergs)
4-0 S(1).....	6370	$4.0 \times 10^{-15}$
8-3 S(2).....	6471	$3.3 \times 10^{-15}$
8-3 S(1).....	6504	$6.7 \times 10^{-15}$
8-3 S(0).....	6551	$4.0 \times 10^{-15}$
8-3 Q(1).....	6658	$4.6 \times 10^{-15}$
5-1 S(3).....	6678	$4.3 \times 10^{-15}$
5-1 S(2).....	6721	$5.2 \times 10^{-15}$
5-1 S(1).....	6779	$8.9 \times 10^{-15}$
5-1 S(0).....	6850	$5.1 \times 10^{-15}$
5-1 Q(1).....	6989	$5.7 \times 10^{-15}$
9-4 S(1).....	7059	$8.7 \times 10^{-15}$
6-2 S(2).....	7181	$8.8 \times 10^{-15}$
6-2 S(1).....	7240	$1.6 \times 10^{-14}$
6-2 S(0).....	7315	$1.0 \times 10^{-14}$
6-2 Q(1).....	7465	$1.3 \times 10^{-14}$
7-3 S(2).....	7709	$1.0 \times 10^{-14}$
10-5 S(1).....	7743	$8.8 \times 10^{-15}$
7-3 S(1).....	7771	$2.1 \times 10^{-14}$
7-3 S(0).....	7850	$1.4 \times 10^{-14}$
3-0 S(3).....	7962	$1.2 \times 10^{-14}$
7-3 Q(1).....	8011	$1.9 \times 10^{-14}$
3-0 S(1).....	8153	$2.5 \times 10^{-14}$
3-0 S(0).....	8275	$1.5 \times 10^{-14}$
8-4 S(1).....	8394	$2.3 \times 10^{-14}$
4-1 S(3).....	8462	$2.1 \times 10^{-14}$
8-4 S(0).....	8477	$1.6 \times 10^{-14}$
3-0 Q(1).....	8500	$2.1 \times 10^{-14}$
4-1 S(2).....	8552	$2.8 \times 10^{-14}$
8-4 Q(1).....	8652	$2.3 \times 10^{-14}$
4-1 S(0).....	8792	$3.2 \times 10^{-14}$
4-1 Q(1).....	9032	$4.6 \times 10^{-14}$
5-2 S(2).....	9116	$3.3 \times 10^{-14}$
5-2 S(1).....	9232	$6.4 \times 10^{-14}$
5-2 S(0).....	9369	$4.3 \times 10^{-14}$
5-2 Q(1).....	9627	$6.7 \times 10^{-14}$
5-2 Q(2).....	9658	$4.0 \times 10^{-14}$
5-2 Q(3).....	9706	$3.4 \times 10^{-14}$
6-3 S(2).....	9758	$3.3 \times 10^{-14}$
6-3 S(1).....	9879	$6.7 \times 10^{-14}$
5-2 O(2).....	9915	$3.6 \times 10^{-14}$
1-0 S(1).....	21218	$4.6 \times 10^{-13}$
Σ (vibrational lines with $\lambda < 1 \mu\text{m}$ ).....		$1.8 \times 10^{-12}$
Σ (all vibrational lines).....		$2.8 \times 10^{-11}$
Σ (1400–1700 Å emission).....		$3.0 \times 10^{-11}$

$I_f$  starts to increase less rapidly<sup>1</sup> than  $N(\text{H})$ , while remaining roughly proportional to  $n_{\text{H}}$ . We note that for given values of  $N(\text{H})$  and  $n_{\text{H}}$ , the fluorescent line intensities show only a weak dependence upon the incident UV continuum flux (although the relationship between  $N(\text{H})$  and  $A_V$  does, of course, depend on  $I_{\text{UV}}$ ).

In Table 1, we present values of the mean energy per photodissociation,  $\bar{E}$ , for several transitions. We list values of  $\bar{E}$  for the strongest 10 lines in each of the 0.6–0.7, 0.7–0.8, 0.8–0.9, and 0.9–1.0  $\mu\text{m}$  ranges, for the  $v = 1-0$  S(1) line, for the sum of all ro-vibrational lines, and for the sum of all electronic transitions within the 1400–1700 Å range. The

<sup>1</sup> In the spherical geometry that we consider,  $I_f$  may even become a decreasing function of  $A_V$  and  $N(\text{H})$  because the cloud becomes optically thick to fluorescent emission generated in surface layers on the far side of the cloud.

results were actually computed for the case in which  $n_{\text{H}} = 100 \text{ cm}^{-3}$ ,  $A_V = 1 \text{ mag}$ , and  $I_{\text{UV}} = 1$ , but were roughly the same for all the model parameters we considered. An approximate fit to absorbed fraction  $f_a$  over the entire parameter space that we considered is provided by the expression

$$1 - f_a = \frac{\{1 - \exp[-\sigma_\lambda N(\text{H})/2]\}}{\sigma_\lambda N(\text{H})} \times \{1 + \exp[\sigma_\lambda N(\text{H})/2 - \sigma_\lambda N_{\text{H}}]\}, \quad (2)$$

where  $\sigma_\lambda$  has the values  $1.43 \times 10^{-21}$ ,  $6.13 \times 10^{-22}$ , and  $1.84 \times 10^{-22} \text{ cm}^2$  at wavelengths of 0.15, 0.72, and 2.12  $\mu\text{m}$ , respectively. Values of  $(1 - f_a)$  given by this expression are typically accurate to better than 15%.

#### 4. DISCUSSION

##### 4.1. Red and Infrared Fluorescent Emissions

The results presented in Figures 1 and 2 suggest that surface brightness sensitivities of order  $4 \times 10^{-8} \text{ ergs cm}^{-2} \text{ s}^{-1} \text{ sr}^{-1}$  will be needed to detect fluorescent 2.122  $\mu\text{m}$  H<sub>2</sub> emission from diffuse clouds with  $n_{\text{H}} = 100 \text{ cm}^{-3}$ ,  $A_V = 1 \text{ mag}$ , and  $I_{\text{UV}} = 1$ . The best sensitivities yet reported (Luhman et al. 1994; Pak et al. 1996) at 2.122  $\mu\text{m}$  are  $\sim 10^{-6} \text{ ergs cm}^{-2} \text{ s}^{-1} \text{ sr}^{-1}$  (1  $\sigma$ ), so a factor  $\sim 50$  improvement would be needed to detect the 2.122  $\mu\text{m}$  for a diffuse cloud with the parameters given above. The required sensitivity for the 7180.5 Å line is  $\sim 40$  times more stringent, yet with the predicted surface brightness being only about  $\sim 10^{-9} \text{ ergs cm}^{-2} \text{ s}^{-1} \text{ sr}^{-1}$ . However, the much lower sky brightness at red visible wavelengths means that observations of the 7180.5 Å line will be considerably more sensitive (cf. BD76). Indeed, Fabry-Perot instruments designed to search for diffuse H $\alpha$  emissions have already demonstrated (Vogel et al. 1995) sensitivities as good as  $\sim 2 \times 10^{-9} \text{ ergs cm}^{-2} \text{ s}^{-1} \text{ sr}^{-1}$  (1  $\sigma$ ), and new instruments under construction are expected to be more sensitive by factors of several (Vogel 1996), suggesting that observations of red H<sub>2</sub> fluorescence from diffuse clouds may soon be within reach. Red H<sub>2</sub> fluorescent emissions are, of course, more severely attenuated than near-infrared emissions by foreground dust. Thus, observations at red visible wavelengths will be limited to nearby or high-latitude clouds, and near-infrared observations will remain essential to probe fluorescent H<sub>2</sub> emission from heavily extinguished regions, such as the Galactic Center (Pak et al. 1996).

We argue that observations of red H<sub>2</sub> fluorescence, combined with H I 21 cm observations, are a potentially valuable probe of conditions in the diffuse interstellar medium. Given a fixed value of  $N(\text{H})$  that has been inferred from 21 cm observations, the fluorescent line intensities are roughly proportional to the product of the rate coefficient for H<sub>2</sub> formation,  $R$ , and the gas density,  $n_{\text{H}}$ , and are only weakly dependent upon  $I_{\text{UV}}$ . Thus, even in the absence of reliable estimates for  $I_{\text{UV}}$ , the product  $Rn_{\text{H}}$  can be determined to reasonable accuracy, subject always to the validity of our assumption of chemical equilibrium. If estimates of  $N(\text{H}_2)$  are also available, then the value of  $I_{\text{UV}}$  can also be determined and the accuracy of the density determination improved, as demonstrated by the analysis in § 4.3 below.

##### 4.2. Scaling Relations

Insofar as collisional excitation may be neglected, it is straightforward to show that the intensity of any fluorescent

line,  $I_f$ , varies with the quantities  $I_{UV}$ ,  $n_H$ ,  $R$ , and  $N(H)$  such that  $I_f/I_{UV}$  is a function of the two variables  $Rn_H/I_{UV}$  and  $N(H)$  alone (cf. discussion in Sternberg 1988). Similarly, the atomic hydrogen column density,  $N(H)$ , is a function of  $A_V$  and  $Rn_H/I_{UV}$  alone.

This scaling is confirmed by our calculations, which show, for example, that the values plotted in Figure 1 for the case  $n_H = 100 \text{ cm}^{-3}$  and  $I_{UV} = 1$  lie exactly a factor of 5 below the values plotted in Figure 2 for the case  $n_H = 500 \text{ cm}^{-3}$  and  $I_{UV} = 5$ , for any value of  $N(H)$  or  $A_V$ . Thus, the results presented in these figures may be used to obtain results for the fluorescent line intensities given values of  $I_{UV}$  (or of the formation rate coefficient  $R$ ) other than those considered in this study. The use of these scalings is illustrated in the discussion of UV fluorescence in § 4.3, with specific application to observations of the Taurus molecular cloud.

### 4.3. Ultraviolet Fluorescence

Figures 1 and 2 indicate that ultraviolet electronic  $H_2$  transitions are considerably more luminous than either near-infrared or red vibrational transitions. The possibility of detecting diffuse ultraviolet fluorescence from interstellar  $H_2$  was first pointed out by Duley & Williams (1980) and investigated further by Jakobsen (1982). Unfortunately, ultraviolet  $H_2$  fluorescence from the diffuse interstellar medium can only be observed from space with the use of telescopes designed to detect faint diffuse UV radiation. Although no such instruments are currently in operation, observations of diffuse ultraviolet emissions from  $H_2$  have been detected in the past.

In particular, MHB90 obtained the first unequivocal<sup>2</sup> detection of ultraviolet  $H_2$  fluorescence from the *diffuse* interstellar medium using the UVX Berkeley Shuttle Spectrometer. MHB90 analyzed the intensity that they observed toward the Taurus molecular cloud, using a theoretical model to investigate the expected dependence of the fluorescent UV intensity upon the  $H_2$  column density,  $N(H_2)$ , and the gas density,  $n_H$ , and reached the conclusion that the observed fluorescent intensity could not be reconciled with the observed values of  $N(H_2)$  and  $N(H)$  on the basis of a homogeneous diffuse cloud model. In particular, given an  $H_2$  column density that they inferred from CO observations to be  $3.4 \times 10^{21} \text{ cm}^{-2}$ , MHB90 concluded that a surprisingly small gas density of only 16 H nuclei per  $\text{cm}^3$  was needed to match the 1400–1700 Å fluorescent intensity on the basis of a homogeneous cloud model, whereas a density  $n_H = 300 \text{ cm}^{-3}$  was needed to explain the atomic hydrogen column density of  $4 \times 10^{20} \text{ cm}^{-2}$ . These values for  $n_H$  were obtained for a particular assumed  $H_2$  formation rate coefficient of  $R = 2 \times 10^{-17} \text{ cm}^3 \text{ s}^{-1}$ , and an investigation of their dependence upon  $R$  indicated that only for an unreasonable small value,  $R = 4 \times 10^{-19} \text{ cm}^3 \text{ s}^{-1}$ , could the two density estimates be reconciled; this led MHB90 to

the conclusion that the observations could only be accommodated by an inhomogeneous cloud model.

We note, however, that MHB90 did not investigate the effect of varying the assumed interstellar UV field,  $I_{UV}$ , but apparently adopted a fixed value for this rather uncertain parameter in all of their calculations. For given values of  $N(H)$  and  $n_H$ , the fluorescent line intensities are indeed predicted to be almost independent of  $I_{UV}$  (see § 3), but in this case the quantities specified by observations were  $N(H)$  and  $N(H_2)$ . If *these* are the two variables that are kept constant, then a dependence upon  $I_{UV}$  does obtain. Thus, Figure 2 in MHB90 applies only to one specific (and unstated) value of  $I_{UV}$  (though results for other values could be obtained by means of the scaling relation discussed in § 4.2). Indeed, when  $N(H_2) \leq 10^{16} \text{ cm}^{-2}$ , the fluorescent intensity plotted in that figure must scale linearly with  $I_{UV}$ .

We have reanalyzed these observations using our fluorescence model to compute the expected UV fluorescent intensity as a function of both  $n_H$  and the incident radiation field,  $I_{UV}$ . With the use of the scaling relations described in § 4.2, we find that the observed values of  $N(H_2)$ ,  $N(H)$ , and  $I_f$  can all be accommodated by a homogeneous cloud model. Given the values inferred by MHB90 for  $N(H_2)$  and  $N(H)$ , we obtain an estimate of 4 for the visual extinction. With the aid of Figure 1 or Figure 2, we find that for this value of  $A_V$  a gas density  $n_H = 125I_{UV}$  is required to match the observed value of  $N(H)$ . For this value of  $n_H/I_{UV}$ , the 1400–1700 Å intensity,  $I_f$ , is found (from either figure) to be given by  $I_f/I_{UV} = 2 \times 10^{-6} \text{ ergs cm}^{-2} \text{ s}^{-1} \text{ sr}^{-1}$ . Comparing this with the observed 1400–1700 Å intensity of  $7 \times 10^{-7} \text{ ergs cm}^{-2} \text{ s}^{-1} \text{ sr}^{-1}$ , we find that the required incident UV intensity is  $I_{UV} = 0.4$ .

Thus, we are able to match all the observations using a homogeneous cloud model in steady state with entirely reasonable parameters<sup>3</sup>:  $I_{UV} = 0.4$  and  $n_H = 50 \text{ cm}^{-3}$ . Discrepancies of the magnitude found by MHB90 would result if the value  $I_{UV} = 2$  were adopted in place of 0.4. Contrary to the conclusions of MHB90, we find that the observed intensities of the  $H_2$  fluorescence from the Taurus molecular cloud do not *require* the presence of inhomogeneities in the fluorescent emission region. Of course, our analysis does not *rule out* the presence of such inhomogeneities.

It is a pleasure to thank J. Black, A. Dalgarno, and A. Sternberg and S. Vogel for helpful discussions. We are particularly grateful to B. Draine for providing us with unpublished results against which our own calculations could be checked. D. A. N. gratefully acknowledges the hospitality of the University of Maryland, College Park, where he was a sabbatical visitor during the period when this study was carried out. We also acknowledge with gratitude the support of NASA grant NAGW-3147 from the Long Term Space Astrophysics Research Program.

<sup>2</sup> Ultraviolet  $H_2$  fluorescence had previously been detected by Witt et al. (1989) from the *dense* ( $n_H \geq 2 \times 10^4 \text{ cm}^{-3}$  according to the analysis of Sternberg 1989), strongly illuminated reflection nebula IC63 using *IUE*.

<sup>3</sup> In deriving these parameters, we assumed an  $H_2$  formation rate coefficient of  $3 \times 10^{-17} \text{ cm}^3 \text{ s}^{-1}$ ; given the smaller value  $R = 2 \times 10^{-17} \text{ cm}^3 \text{ s}^{-1}$  adopted by MHB90, the solution would be  $I_{UV} = 0.4$  and  $n_H = 75 \text{ cm}^{-3}$ .

### REFERENCES

Beckwith, S., Persson, S. E., Neugebauer, G., & Becklin, E. E. 1978, ApJ, 223, 464  
Black, J. H., & Dalgarno, A. 1976, ApJ, 203, 132 (BD76)

Black, J. H., & van Dishoeck, E. F. 1987, ApJ, 322, 412 (BvD87)  
Burton, M. G., Bulmer, M., Moorhouse, A., Geballe, T. R., & Brand, P. W. J. L. 1992, MNRAS, 257, 1P

- Chernoff, D. F., Hollenbach, D. J., & McKee, C. F. 1982, *ApJ*, 259, L97  
Chrysostomou, A., Brand, P. W. J. L., Burton, M. D., & Moorhouse, A. 1993, *MNRAS*, 265, 329  
Dalgarno, A. 1996, private communication  
Doyon, R., Wright, G. S., & Joseph, R. D. 1994, *ApJ*, 421, 115  
Draine, B. T. 1978, *ApJS*, 36, 595  
Draine, B. T., & Bertoldi, F. 1996, *ApJ*, 468, 269 (DB96)  
Draine, B. T., & Roberge, W. G. 1982, *ApJ*, 259, L91  
Duley, W. W., & Williams, D. A. 1980, *ApJ*, 242, L179  
Field, G. B., Somerville, W. B., & Dressler, K. 1966, *ARA&A*, 4, 226  
Gatley, I., et al. 1987, *ApJ*, 318, L73  
Goldshmidt, O., & Sternberg, A. 1995, *ApJ*, 439, 256  
Gould, R. J., & Harwit, M. 1963, *ApJ*, 137, 694  
Gull, T. R., & Harwit, M. 1971, *ApJ*, 168, 15  
Hippelein, H. H., & Münch, G. 1989, *A&A*, 187, 581  
Jakobsen, P. 1982, *A&A*, 106, 375  
Kawara, K., Nishida, M., & Gregory, B. 1987, *ApJ*, 321, L35  
Lepp, S., Buch, V., & Dalgarno, A. 1995, *ApJS*, 98, 345  
Luhman, M. L., Jaffe, D. T., Keller, L. D., & Pak, S. 1994, *ApJ*, 436, L185  
Martin, C., Hurwitz, M., & Bowyer, S. 1990, *ApJ*, 354, 220 (MHB90)  
Münch, G., Hippelein, H. H., & Pitz, 1984, *A&A*, 135, L11  
Pak, S., Jaffe, D. T., & Keller, L. D. 1996, *ApJ*, 457, L43  
Savage, B. D., Bohlin, R. C., Drake, J. F., & Budich, W. 1977, *ApJ*, 216, 291  
Shull, J. M., & Beckwith, S. 1982, *ARA&A*, 20, 163  
Stecher, T. P., & Williams, D. A. 1967, *ApJ*, 149, L29  
Stephens, T. L., & Dalgarno, A. 1972, *J. Quant. Spectrosc. Radiat. Transfer*, 12, 569  
Sternberg, A. 1988, *ApJ*, 332, 400  
———. 1989, *ApJ*, 347, 863  
Sternberg, A., & Dalgarno, A. 1989, *ApJ*, 338, 197 (SD89)  
Störzer, H., Stutzki, J., & Sternberg, A. 1996, *A&A*, 310, 592  
Tielens, A. G. G. M., & Hollenbach, D. 1985, *ApJ*, 291, 722  
Traub, W. A., Carleton, N. P., Black, J. H. 1978, *ApJ*, 223, 140  
Turner, J., Kirby-Docken, K., & Dalgarno, A. 1977, *ApJS*, 35, 281  
Vogel, S. N. 1996, private communication  
Vogel, S. N., Weymann, R., Rauch, M., & Hamilton, T. 1995, *ApJ*, 441, 162  
Witt, A. N., Stecher, T. P., Boronson, T. A., & Bohlin, R. C. 1989, *ApJ*, 336, L21